Geoscience Frontiers xxx (2016) 1–10

HOSTED BY

ELSEVIER

Contents lists available at ScienceDirect

China University of Geosciences (Beijing)

Geoscience Frontiers

journal homepage: www.elsevier.com/locate/gsf

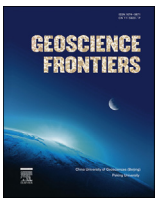

Research paper

Reactions between olivine and CO_2-rich seawater at 300 °C: Implications for H_2 generation and CO_2 sequestration on the early Earth

Hisahiro Ueda [a,*], Yusuke Sawaki [a], Shigenori Maruyama [b]

[a] Department of Earth and Planetary Sciences, Tokyo Institute of Technology, 2-12-1 Ookayama, Meguro-ku, Tokyo 152-8551, Japan
[b] Earth-Life Science Institute, Tokyo Institute of Technology, 2-12-1 Ookayama, Meguro-ku, Tokyo 152-8551, Japan

ARTICLE INFO

Article history:
Received 31 March 2016
Received in revised form
17 September 2016
Accepted 3 October 2016
Available online xxx

Keywords:
Olivine
CO_2-rich condition
Early Earth
Hydrothermal alteration
Serpentinization
Experiment

ABSTRACT

To understand the influence of fluid CO_2 on ultramafic rock-hosted seafloor hydrothermal systems on the early Earth, we monitored the reaction between San Carlos olivine and a CO_2-rich NaCl fluid at 300 °C and 500 bars. During the experiments, the total carbonic acid concentration (ΣCO_2) in the fluid decreased from approximately 65 to 9 mmol/kg. Carbonate minerals, magnesite, and subordinate amount of dolomite were formed via the water-rock interaction. The H_2 concentration in the fluid reached approximately 39 mmol/kg within 2736 h, which is relatively lower than the concentration generated by the reaction between olivine and a CO_2-free NaCl solution at the same temperature. As seen in previous hydrothermal experiments using komatiite, ferrous iron incorporation into Mg-bearing carbonate minerals likely limited iron oxidation in the fluids and the resulting H_2 generation during the olivine alteration. Considering carbonate mineralogy over the temperature range of natural hydrothermal fields, H_2 generation is likely suppressed at temperatures below approximately 300 °C due to the formation of the Mg-bearing carbonates. Nevertheless, H_2 concentration in fluid at 300 °C could be still high due to the temperature dependency of magnetite stability in ultramafic systems. Moreover, the Mg-bearing carbonates may play a key role in the ocean-atmosphere system on the early Earth. Recent studies suggest that the subduction of carbonated ultramafic rocks may transport surface CO_2 species into the deep mantle. This process may have reduced the huge initial amount of CO_2 on the surface of the early Earth. Our approximate calculations demonstrate that the subduction of the Mg-bearing carbonates formed in komatiite likely played a crucial role as one of the CO_2 carriers from the surface to the deep mantle, even in hot subduction zones.

1. Introduction

Fluids circulating through ultramafic rocks are usually rich in reduced volatile constituents such as hydrogen and methane molecules (e.g., Neal and Stanger, 1983; Charlou et al., 2002, 2010; Etiope et al., 2011, 2016). These compounds could be important to sustain ecosystems, including chemolithoautotrophic microorganisms on the early Earth (e.g., Amend and McCollom, 2009; Russell et al., 2014). Even though hydrogen molecules provide the foundation for prebiotic chemical evolution and early energy metabolisms, the chemical reactions that regulate H_2 production remain uncertain. It is widely accepted that H_2 generation is tightly coupled with the oxidation of ferrous iron to ferric iron in parallel with the reduction of water molecule (e.g., Allen and Seyfried, 2003; Seyfried et al., 2007; McCollom and Bach, 2009). Multiple factors controlling H_2 generation have been suggested by previous studies such as the iron content of source minerals, the aluminum content of ultramafic rocks, the activity of silica, and the thermodynamic equilibrium between the mineral phases (e.g., McCollom and Bach, 2009; Klein et al., 2013; Shibuya et al., 2015).

Numerical modeling (Walker, 1985; Kasting, 1993; Elkins-Tanton, 2008) and geological records (Lowe and Tice, 2004; Ohmoto et al., 2004; Shibuya et al., 2007, 2012) indicate that atmospheric CO_2 levels on the early Earth were likely much higher than the present levels. Carbonate formation during the

* Corresponding author. Fax: +81 3 5734 3538.
E-mail address: ueda.h.ai@m.titech.ac.jp (H. Ueda).
Peer-review under responsibility of China University of Geosciences (Beijing).

http://dx.doi.org/10.1016/j.gsf.2016.10.002

Please cite this article in press as: Ueda, H., et al., Reactions between olivine and CO_2-rich seawater at 300 °C: Implications for H_2 generation and CO_2 sequestration on the early Earth, Geoscience Frontiers (2016), http://dx.doi.org/10.1016/j.gsf.2016.10.002

serpentinization of olivine under CO_2-rich conditions likely suppresses H_2 generation in fluids (Jones et al., 2010; Klein and McCollom, 2013; Neubeck et al., 2014); however, these studies examined temperature ranges up to 230 °C. McCollom et al. (2016) also conducted hydrothermal experiments using San Carlos olivine under CO_2-rich conditions (approximately 20 mmol/kg CO_2) at various temperatures up to 320 °C and emphasized the importance of temperature and iron partitioning for H_2 generation. However, due to the minor contribution of precipitated carbonate to the total mass balance, the influence of CO_2 on H_2 generation was not fully discussed in their study. Because the H_2 production rate derived from olivine hydration is greatest near 300 °C based on model calculations (Klein et al., 2013), the serpentinization of olivine under highly CO_2-rich conditions at such high temperatures should be tested via laboratory experiments.

Addition of carbon dioxide into experimental system has other key aspects. In the methane and hydrocarbons in the Rainbow and Lost City hydrothermal fields may have an abiotic origin (Charlou et al., 2002, 2010; Proskurowski et al., 2008), which could be important for the abiotic synthesis of building blocks on the early Earth. The production of abiotic methane possibly occur in association with Fischer-Tropsch-type reactions between molecular hydrogen from serpentinization and carbon compounds, such as CO_2 (Etiope and Sherwood Lollar, 2013), or direct olivine hydration in the presence of CO_2 (Oze and Sharma, 2005). However, recent hydrothermal experiments have demonstrated that significant amounts of methane are not generated by low temperature (50 °C) olivine hydration in CO_2-rich fluid (Neubeck et al., 2016.). Experiment in this study examines the possibility of methane production at higher temperature (300 °C). In the meanwhile, the early atmosphere may have contained all the Earth's carbon, corresponding to a partial pressure on the order of 10–340 MPa (Liu, 2004; Elkins-Tanton, 2008). If the majority of the carbon was in the early atmosphere, there must have existed large-scale carbon removal processes at a later time. On time scales of billions of years, the subduction of carbonated oceanic crust has the potential to transport carbon from the Earth's surface to its interior (Fig. 1). In current subduction zones, carbon in the crust remains stable as calcite during shallow dehydration and possibly hydrous melting according to phase equilibrium experiments (Yaxley and Green, 1994; Molina and Poli, 2000; Poli et al., 2009) and thermodynamic calculations (Kerrick and Connolly, 2001; Connolly, 2005). Moreover, the modern subduction of oceanic crust likely transports carbon into the deep mantle in the form of carbonated eclogite (Dasgupta et al., 2005). Sleep and Zahnle (2001) proposed catastrophic carbon removal from the ocean-atmosphere system via this process soon after solidification of the magma ocean. However, in the hot subduction zones on the early Earth, carbonate was likely released at shallow depths and might largely return to the atmosphere (Dasgupta and Hirschmann, 2010). Other mechanisms have been suggested to introduce carbon into the mantle, such as the subduction of (1) reduced carbon species such as graphite, (2) carbonate sequestered in deep subducting plates as altered peridotite, and (3) carbon trapped in lithospheric overriding plates (Sleep, 2009; Dasgupta and Hirschmann, 2010). Carbonate rocks on continents likely were minor prior to 2.0 Ga (Ronov, 1964; Veizer et al., 2003) and therefore could not account for a large inventory of carbon on the early Earth. Thermodynamic calculations indicate that Mg-bearing carbonate minerals are more stable than Ca-carbonate minerals in subduction P-T conditions on the early Earth (Aral et al., this volume). We focus on carbonate mineralogy formed in ultramafic rocks and its ability to remove CO_2 from the ocean-atmosphere system.

We performed a hydrothermal experiment to monitor the reactions between olivine and CO_2-rich seawater at 300 °C and 500 bars using a batch-type (closed system) hydrothermal reactor (Yoshizaki et al., 2009). The aims of this study are (1) to determine the quantities of hydrogen and methane molecules and (2) to determine the CO_2 absorption ability of ultramafic rocks via serpentinization under CO_2-rich conditions.

2. Sample preparation and experimental procedure

2.1. Starting material

Only olivine crystals from San Carlos (Arizona) were used in this experiment, and they were handpicked to exclude grains with obvious signs of weathering or inclusions of other minerals. The composition of the olivine was analyzed using an electron probe micro analyzer (EPMA). The analytical conditions for the EPMA were an accelerating voltage of 15 kV, a specimen current of 10 nA, and a counting time of 60–80 s. The results indicate that the olivine crystals have $Mg^{\#}$ values ($Mg^{\#} = 100 \times Mg/(Mg + Fe)$) ranging from 90 to 91 (Table 1). The olivine was crushed in an agate-ball mill and

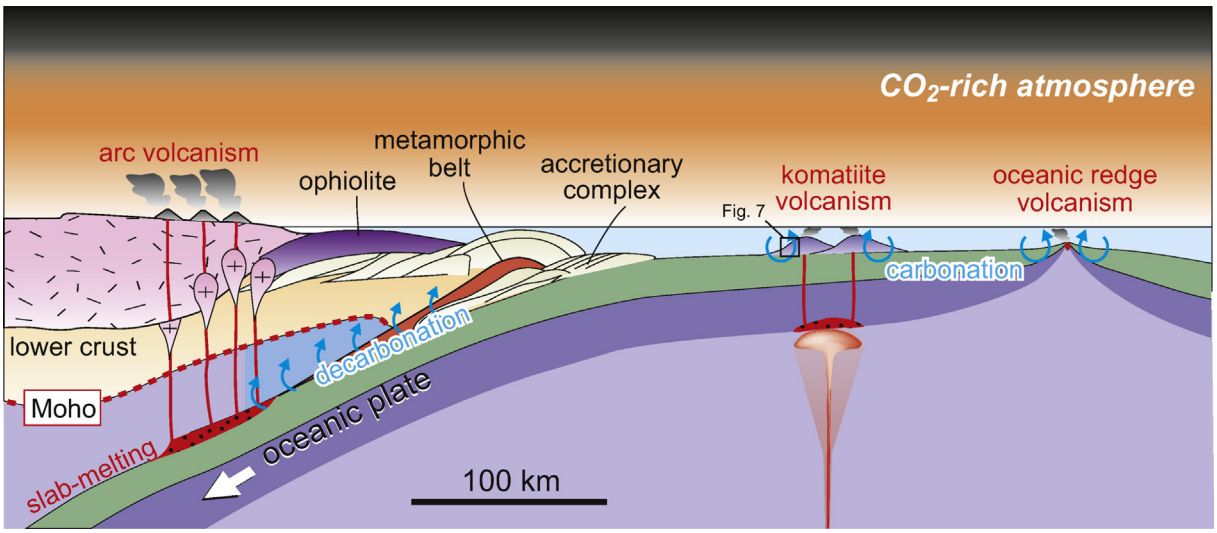

Figure 1. Schematic of surface environment on the early Earth. Under CO_2-rich conditions, carbonation of oceanic crust occurs in hydrothermal systems. The oceanic crust releases some amount of carbon (decarbonation) at the subduction zone depending on its P-T trajectory and carbonate mineralogy.

Please cite this article in press as: Ueda, H., et al., Reactions between olivine and CO_2-rich seawater at 300 °C: Implications for H_2 generation and CO_2 sequestration on the early Earth, Geoscience Frontiers (2016), http://dx.doi.org/10.1016/j.gsf.2016.10.002

Table 1
Major element compositions of the San Carlos olivine used in this study (wt.%).

	XRF	EPMA		
SiO_2	38.63	41.47	41.67	41.71
TiO_2	0.01	0.00	0.00	0.00
Al_2O_3	0.14	0.00	0.05	0.01
Fe_2O_3	11.18			
FeO		8.47	9.25	9.15
MnO	0.16	0.09	0.12	0.07
MgO	49.07	49.48	49.37	49.52
CaO	0.20	0.07	0.08	0.08
Na_2O	0.43	0.00	0.00	0.06
K_2O	0.01	0.00	0.00	0.07
P_2O_5	BDL	NA	NA	NA
NiO	NA	0.35	0.35	0.35
Total	99.82	99.92	100.88	101.02
$Mg^{\#}$[a]	0.90	0.91	0.90	0.91

BDL, below detection limit; NA, not analyzed.
[a] $Mg^{\#} = [Mg/(Mg + Fe)] \times 100$.

sieved to obtain a >100 μm powder. To remove any contamination of organic materials during sample preparation, the powdered olivine was pre-sintered for 12 h in an oven at 450 °C. The composition of the powdered olivine was analyzed via X-ray fluorescence (XRF). Prior to preparing the fused glass discs, the rock powders were heated at 950 °C for 24 h. The glass discs were made with a lithium tetraborate flux ($Li_2B_4O_7$) with a dilution ratio of 1:10 at 1050 °C. Major element compositions were determined from the fused glass discs using an X-ray fluorescence spectrometer (RIX 2100, RIGAKU) at the Tokyo Institute of Technology, Japan. The accelerating voltage and current were 50 kV and 50 mA, respectively. Repeated analyses of the same standard indicated that the reproducibility of this analysis was better than 1%, except for Na and P (<5%). This result confirmed that the $Mg^{\#}$ value of the powdered olivine is 90 and that contamination other than olivine was minor (Table 1).

2.2. Experimental system

The Inconel alloy autoclave for the hydrothermal experiment is modeled after the study of Seyfried et al. (1979). This device resists salt corrosion and withstands high temperature and pressure conditions. The reaction cell is made of a gold bag with a titanium head. The gold is resistant to high-temperature fluids and has sufficient flexibility to allow the fluid inside the reaction cell to be pressurized by the surrounding water. To reduce H_2 generation via the reaction of the metallic titanium head with the fluids, the surface of the titanium was fully oxidized before the hydrothermal experiment. A blank experiment without olivine revealed that the H_2 concentration after 2184 h was 0.004 mmol/kg, which is sufficiently low for this study. To eliminate contamination of organic matter, all apparatus in contact with the sample fluid were baked in a muffle furnace at 450 °C for more than 12 h.

The initial solution used in the experiments was regulated via the addition of NaCl (99.5% purity, Wako Pure Chemical Industries, Ltd.) to ultrapure water. The Cl concentration of the solution was adjusted to be approximately 550 mmol/kg, which is equivalent to modern values. ^{13}C-labeled gaseous CO_2 was introduced into the reaction cell directly from a gas cylinder because previous studies have suggested that atmospheric CO_2 levels were likely much higher in the past (e.g., Kasting, 1993; Macleod et al., 1994). The resulting $\Sigma CO_2 (= CO_{2\ (aq)} + HCO_3^- + CO_3^{2-})$ concentration in the fluid was maintained at approximately 65 mmol/kg. The 12 g of olivine powder was reacted with this hypothetical seawater in the reaction cell at 300 °C and 500 bars for 2736 h. At the beginning of the experiments, the water/rock mass ratio was set to approximately 5, similar to values seen in high-temperature regions of modern sub-seafloor hydrothermal systems (Wetzel and Shock, 2000). Due to the multiple fluid samplings during the experiments, this ratio decreased to approximately 3 by the end of the experiments.

2.3. Sampling and analytical methods

During the experiments, fluid samples of approximately 3 g were collected several times via a sampling tube, the inside of which was coated with gold. For the H_2 and CO_2 analyses, a 0.5 mL fluid sample was directly introduced into each He-purged, sealed vial at room temperature. After measuring the H_2, to determine the ΣCO_2 concentration in the fluid, the sampled fluid was acidified (pH < 2) with HCl to accomplish the complete extraction of the dissolved bicarbonate and carbonate ions. A quantitative analysis of the gas species was conducted using a Tracera GC-2010 Plus gas chromatograph (Shimadzu Corporation, Japan) with a barrier discharge ionization detector (BID). The procedural precisions of the analyses of the ΣCO_2 and H_2 concentrations in the fluid were better than 5%. For the analysis of the dissolved species, 0.2 mL of the fluid was collected in two vials. The Cl^- and Na^+ concentrations in the fluid samples were measured using ion chromatography (Shimadzu, Prominence HIC-NS/SP model). The analytical reproducibility (2σ) was better than 2% for K and 1% for the other elements. We made a mistake in the dilution of the sampling fluid for the cation analysis at 240 h and the anion analyses at 600 and 1152 h; therefore, these data are shown as white circles in Fig. 2a. We obtained the other cation abundances (Mg, K, Ca, Si, Fe, and Mn) using an inductively coupled plasma-optical emission spectrometer (ICP-OES, LEEMANS Labs. Ink., Prodigy) at the Center for Advanced Materials Analysis in the Tokyo Institute of Technology, Japan. The pH of the fluid samples was measured using a pH meter at 25 °C under atmospheric conditions 1 h after sampling, which allowed for the stabilization of the pH against CO_2 degassing.

Following the experiments, the altered powder sample was extracted from the reaction cell and dehydrated at 80 °C for 12 h. The dried alteration products were mounted in Epofix resin and used to make thin sections. The polished surfaces of the individual alteration minerals were analyzed using EPMA to determine the mineral assemblage and their chemical compositions. Elemental maps were acquired using a Hitachi S-3400N scanning electron microscope (SEM; Hitachi High Tech. Corp., Japan) with an energy-dispersive X-ray spectroscope (EDS; Bruker Corp., USA). To roughly quantify the amount of each mineral, the dried powder sample was analyzed using XRD (X-ray powder diffraction).

3. Results

3.1. Fluid chemistry

The Na and Cl concentrations in the fluid kept relatively constant throughout the experiment (Fig. 2a and Table 2). In general, Cl-bearing minerals are minor constituents in hydrothermally altered rocks, which accounts for the stable Cl concentration. By contrast, the concentrations of other elements (K, Mg, Ca, Fe, and Si) decreased 24 h after the beginning of the experiment. The Mg and Ca concentrations decreased from 0.87 mmol/kg to 0.02 mmol/kg and from 0.75 mmol/kg to 0.09 mmol/kg, respectively. The $m_{Mg}/(m_{Mg} + m_{Ca})$ ratios in the fluid also decreased from approximately 0.56 to 0.19. The high K and Mg contents at 0 h are likely due to elution from the NaCl reagent (99.5% purity). The dissolved Si and Fe concentrations in fluid decreased to approximately 0.01 mmol/kg in the final analysis.

Please cite this article in press as: Ueda, H., et al., Reactions between olivine and CO_2-rich seawater at 300 °C: Implications for H_2 generation and CO_2 sequestration on the early Earth, Geoscience Frontiers (2016), http://dx.doi.org/10.1016/j.gsf.2016.10.002

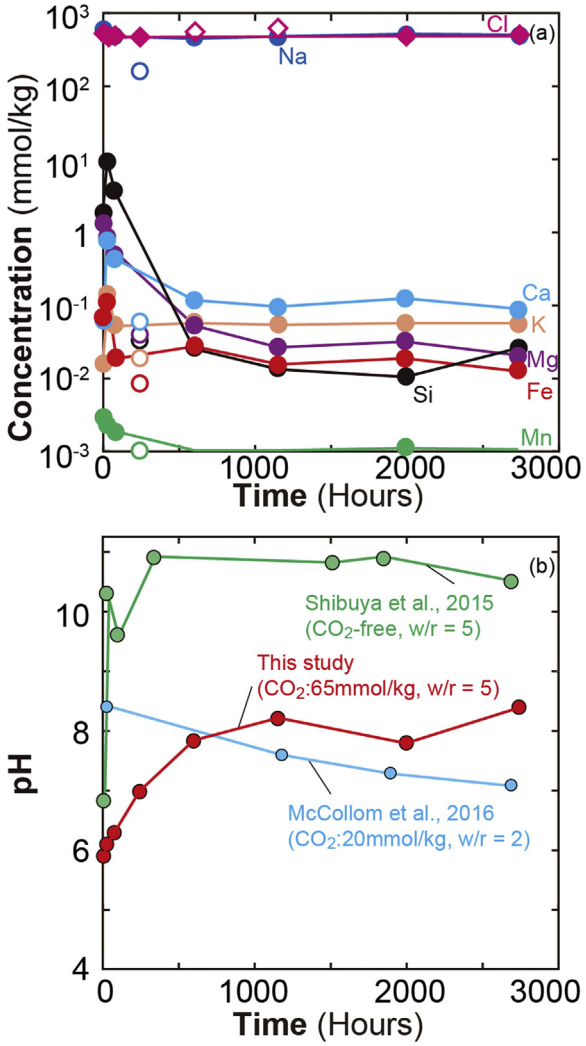

Figure 2. (a) Concentrations of dissolved species in an aqueous fluid coexisting with olivine powder and its alteration products as a function of reaction time in experiment at 300 °C and 500 bars. Cation data at 240 h are expressed as white circles due to a mistake in the dilution of sampling fluid. (b) Temporal variations of pH in this and previous studies (Shibuya et al., 2015; McCollom et al., 2016), all of which performed hydrothermal experiments using olivine at 300 °C. w/r: water/rock mass ratio.

The ΣCO_2 concentration in the fluid decreased from approximately 64.8 mmol/kg at 24 h after the beginning of the experiments to approximately 9.9 mmol/kg within 2736 h (Fig. 3a and Table 2). As the reaction proceeded, the $pH_{25\ ^\circ C}$ values varied from 5.9 to 8.4 (Fig. 2b). The H_2 concentration in the fluid monotonously increased up to approximately 38.9 mmol/kg at 2736 h (Fig. 3b). Trivial amounts of methane (0.03–0.20 mmol/kg) were detected in fluids, likely representing contamination by atmospheric CH_4 during the syringe injection. Therefore, we could not identify with certainty the amount of methane formed under the experimental conditions used in this study.

3.2. Run products

The San Carlos olivine crystal used in this study was altered through the experiments, which is evident when observing the alteration products (Fig. 4a). Serpentine, brucite, and olivine were dominant in the run products. The chemical compositions of the olivine in the alteration products are similar to those of the unaltered olivine (Tables 1 and 3). The $Mg^{\#}$ values of the serpentine (90–97) and brucite (93–95) were higher than those in the olivine (approximately 90–91; Table 3). Magnesite and dolomite were identified as the carbonate minerals, and both minerals displayed euhedral shapes (Fig. 4b). Compositional zoning of Fe was observed in some magnesite grains (Fig. 4c–f). The FeO_{total} values in the magnesite and dolomite are 2.1–8.6 wt.% and 0.6 wt.%, respectively (Table 3). Many magnetite grains, less than 10 μm in diameter, are scattered throughout the run products (Fig. 4a and Table 3). The occurrence of serpentine and carbonate minerals in the run products suggests that the olivine was altered by both serpentinization and carbonation.

The XRD analysis shows that brucite, olivine, and serpentine were abundant in the run products (Fig. 5), which is consistent with the EPMA observations (Fig. 4a). Slight peaks of magnesite were recognizable, but no peaks of dolomite and magnetite were obtained (Fig. 5).

4. Discussion

4.1. Nature of the serpentinization and carbonation of olivine under CO_2-rich conditions

The ΣCO_2 concentrations in the fluids decreased from approximately 65 to 9 mmol/kg (Fig. 3a), indicating that carbonate minerals formed as the reaction progressed. The run products included magnesite and dolomite as carbonate minerals (Fig. 4); however, the amount of the former was larger than that of the latter based on the XRD analysis (Fig. 5). Under CO_2-rich conditions, Mg-bearing carbonate minerals, such as magnesite and dolomite, are commonly identified in alteration products formed from olivine (e.g. Klein and McCollom, 2013; McCollom et al., 2016). In addition, it has been suggested that the precipitated carbonate species depends on the concentration ratio between Mg and Ca ($m_{Mg^{2+}}/(m_{Mg^{2+}} + m_{Ca^{2+}})$) and the temperature of the fluid (Fig. 6; Rosenberg and Holland, 1964, Rosenberg et al., 1967; Tribble et al., 1995). In this experiment, the $m_{Mg^{2+}}/(m_{Mg^{2+}} + m_{Ca^{2+}})$ values of the fluid range from 0.32 to 0.55 in the period between 0 h and 600 h and from 0.19 to 0.23 in

Table 2
Composition of the sampled fluids in the experiments at 300 °C and 500 bars (mmol/kg).

Experiment	Time (h)	$pH_{25\ ^\circ C}$[a]	H_2	ΣCO_2[b]	CH_4	Cl	Na	K	Mg	Ca	Si	Fe	Mn
Olivine-CO_2	0	5.9	0.04	46.4	0.07	538.0	609.4	0.02	1.34	0.06	0.43	0.06	0.003
	24	6.1	0.51	64.8	0.20	466.4	513.0	0.14	0.87	0.75	1.55	0.11	0.002
	72	6.3	0.39	42.6	0.18	488.0	495.2	0.05	0.50	0.41	0.73	0.02	0.002
	240	7.0	1.81	15.4	0.08	471.9	164.1	0.02	0.04	0.06	0.02	0.01	<0.001
	600	7.8	7.05	9.4	0.03	563.9	477.8	0.06	0.06	0.12	0.01	0.02	0.001
	1152	8.2	13.09	9.4	0.13	630.7	482.7	0.06	0.03	0.09	0.01	0.02	0.001
	1992	7.8	24.32	8.4	0.08	493.9	542.5	0.06	0.03	0.12	0.01	0.02	0.001
	2736	8.4	38.85	9.9	0.06	516.2	534.4	0.06	0.02	0.09	0.01	0.01	0.001

[a] Measured pH after CO_2 degassing.
[b] Measured ΣCO_2 concentration after CO_2 degassing.

Please cite this article in press as: Ueda, H., et al., Reactions between olivine and CO_2-rich seawater at 300 °C: Implications for H_2 generation and CO_2 sequestration on the early Earth, Geoscience Frontiers (2016), http://dx.doi.org/10.1016/j.gsf.2016.10.002

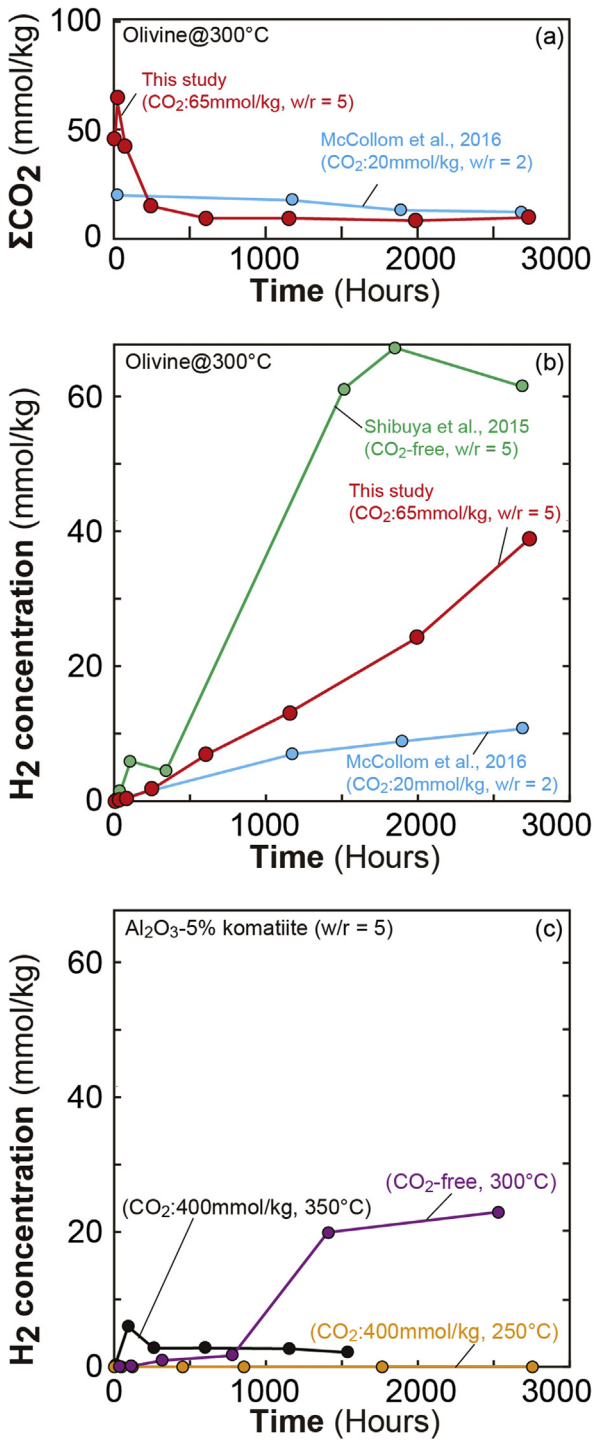

Figure 3. Temporal changes in (a) the dissolved ΣCO_2 and (b and c) the H_2 concentrations in the fluids. Data plotted in (b) are from hydrothermal experiments using olivine at 300 °C (Shibuya et al., 2015; McCollom et al., 2016), whereas those in (c) are from hydrothermal experiments using komatiite including 5 wt% Al_2O_3 (Shibuya et al., 2015; Ueda et al., 2016). w/r: water/rock mass ratio.

the period between 1152 h and 2736 h. These values fall within the stability field of magnesite and dolomite (Fig. 6), which is consistent with SEM-EDS observations (Fig. 4b).

The ΣCO_2 concentrations in the fluids after 600 h in this study were lower than those in a similar hydrothermal experiment by McCollom et al. (2016), although the former (65 mmol/kg) includes more ΣCO_2 than the latter (20 mmol/kg) at the beginning of the experiments (Fig. 3a). As mentioned in McCollom et al. (2016), most of the olivine in the reaction cell (~3%) remained un-reacted at the end of the previous experiment. This fact accounts for the relatively invariant ΣCO_2 concentration in previous work. On the other hand, judging from the relative peak intensities in the XRD patterns (Fig. 5b), substantial amounts of brucite and serpentine exist in the alteration products compared to olivine. Therefore, the difference in the reduced ΣCO_2 between this study and McCollom et al. (2016) is possibly attributed to amounts of the reacted olivine.

Except for carbonate minerals, serpentine, brucite, olivine, and magnetite were observed in the run products (Fig. 4a and Table 3). This mineral assemblage and the $Mg^{\#}$ values in the serpentine and brucite are similar to those predicted from thermodynamic calculations simulating the serpentinization of olivine at 300 °C under CO_2-free conditions by Klein et al. (2013) (Fig. 7a). Low Si concentrations in fluids (<0.02 mmol/kg; Table 2) are consistent with the occurrence of brucite. Previous experiments demonstrated that Mg-bearing carbonate minerals are more stable than brucite under CO_2-rich conditions (Zhao et al., 2010; Hövelmann et al., 2012; Klein and McCollom, 2013), but both brucite and magnesite were observed in this study (Table 3). The initial ΣCO_2 concentration in this study (approximately 65 mmol/kg) is low compared to these previous studies (up to 1200 mmol/kg), which likely decreases the amount of carbonate minerals and may enable brucite formation. Therefore, the coexistence of brucite and magnesite in this study is likely explained by the relatively low ΣCO_2 concentrations.

The $pH_{25\,°C}$ values of the fluids in the presented experiment are clearly lower than those in a similar experiment that was conducted under the CO_2-free condition (Fig. 2b; Shibuya et al., 2015). In this experiment, gaseous CO_2 was injected into the reaction cell and was dissolved into the hypothetical seawater. The carbonate species likely decreased the pH value via the following reaction.

$$CO_{2\,(aq)} + H_2O \leftrightarrow HCO_3^- + H^+ \leftrightarrow CO_3^{2-} + 2H^+$$

The $pH_{25\,°C}$ values in this study changed toward alkaline with increasing reaction time (8.4 at 2736 h). This increasing pH trend parallels that observed in the CO_2-free experiment by Shibuya et al. (2015) and resulted from progress of water/rock reaction. On the other hand, $pH_{25\,°C}$ values of an experiment that included 20 mmol/kg ΣCO_2 in the fluid displayed the opposite trend (McCollom et al., 2016). This likely resulted from insufficient levels of olivine reaction, as mentioned above, as can be attested by the fact that little alkaline and alkaline metal elements were dissolved in the fluids in the previous experiment.

4.2. *Effect of seawater CO_2 on H_2 concentrations in fluids*

Some experimental studies have reported that H_2 is generated by reactions between olivine and H_2O under hydrothermal conditions (e.g., Berndt et al., 1996; Allen and Seyfried, 2003; Shibuya et al., 2015). H_2 generation is caused by ferrous iron oxidation to ferric iron in conjunction with the reduction of H_2O. The higher $Mg^{\#}$ values of serpentine and brucite compared to olivine (Table 3) indicate ferrous iron dissolution, some of which is converted into ferric iron and exists as magnetite in alteration products.

Shibuya et al. (2015) used San Carlos olivine for their hydrothermal experiment at 300 °C under the CO_2-free condition and showed H_2 concentrations in fluids reaching approximately 60 mmol/kg. On the other hand, the maximum H_2 concentrations generated by the hydrothermal alteration of San Carlos olivine under CO_2-rich conditions (McCollom et al., 2016; this study) are lower than this value (Fig. 3b). The experimental conditions in this study and Shibuya et al. (2015) are the same, except for the CO_2, thus it is likely that fluid CO_2 suppresses H_2 generation during

Please cite this article in press as: Ueda, H., et al., Reactions between olivine and CO_2-rich seawater at 300 °C: Implications for H_2 generation and CO_2 sequestration on the early Earth, Geoscience Frontiers (2016), http://dx.doi.org/10.1016/j.gsf.2016.10.002

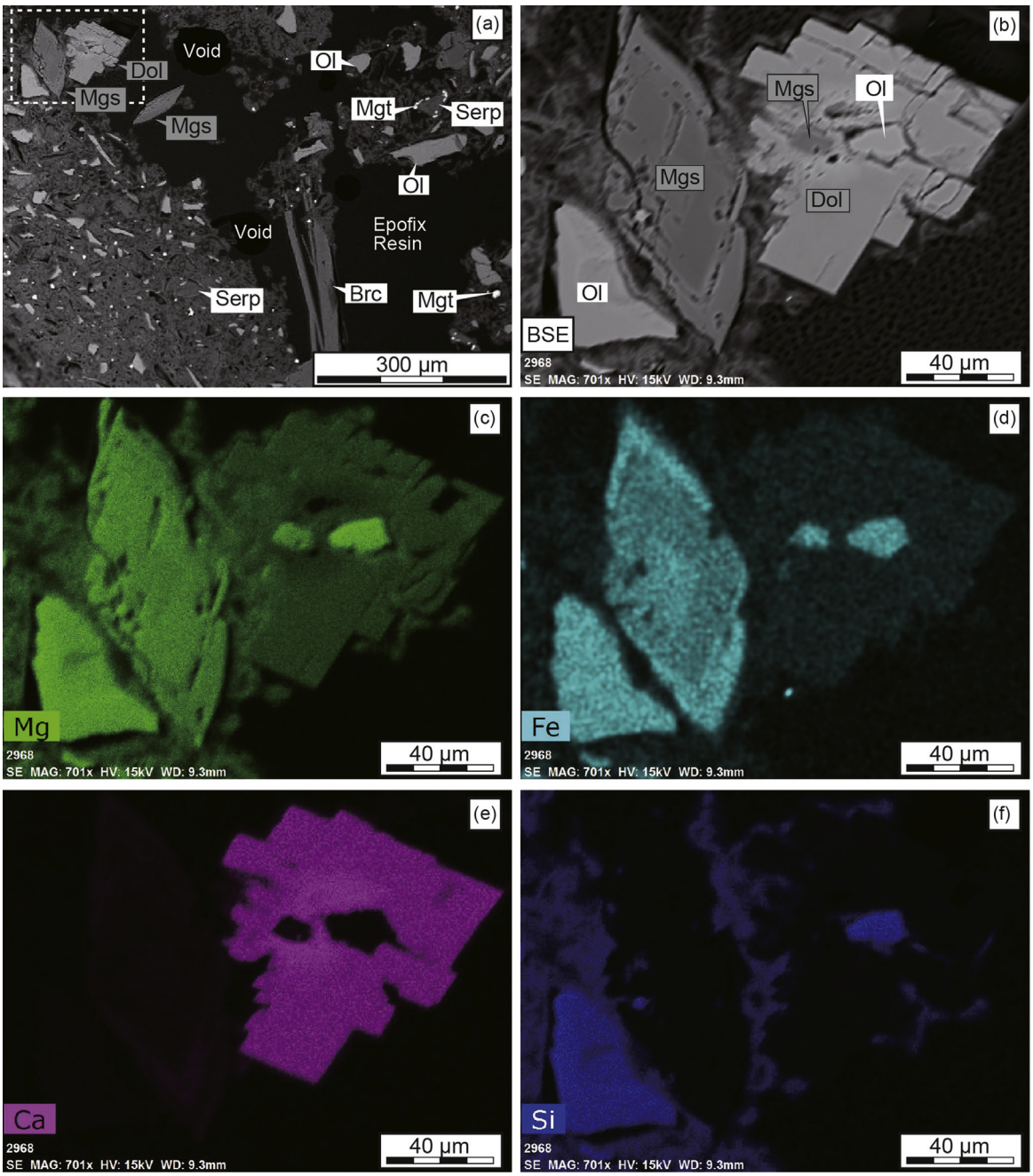

Figure 4. Representative BSE images and elemental maps obtained with SEM-EDS for the alteration products. The white square with a dotted line in (a) marks the position of the images (b)–(f). Mgs: Magnesite, Dol: Dolomite, Ol: Olivine, Serp: Serpentine, Brc: Brucite, and Mag: Magnetite.

water/rock reactions. The major precipitated carbonate mineral through this experiment was magnesite, as seen in the reaction products in McCollom et al. (2016). Because Fe^{2+} often substitutes for Mg^{2+} in the crystal lattice due to their similar charges and ionic radii, iron released from olivine can be incorporated into carbonate minerals without oxidation to ferric iron. In actuality, the magnesite in the run products includes a certain amount of Fe, whose content (FeO_{total}) ranges from 2.1 to 8.6 wt.% (Table 3), and it is likely that this ferrous iron involvement prevented H_2 generation. Trends indicating that iron-bearing carbonates suppress H_2 production have been shown in hydrothermal experiments using olivine (Jones et al., 2010; Klein and McCollom, 2013) and komatiite (Fig. 3c; Ueda et al., 2016) under 250 °C. Meanwhile, maximum H_2 concentration in this study was higher than that in an experiment (Fig. 3b) where olivine reacted with a fluid containing 20 mmol/kg ΣCO_2 at 300 °C and 500 bars (McCollom et al., 2016). This cannot be explained by differences in the initial ΣCO_2 concentrations and water/rock ratios because both parameters in this study are expected to result in a lower H_2 concentration than the previous study. As mentioned above, this is also related to the fact that a large fraction of olivine remained at the termination of the experiment by McCollom et al. (2016).

When considering H_2 generation at higher temperature, the temperature dependency of the stability of magnetite in ultramafic systems is another important factor. Based on thermodynamic calculations (McCollom and Bach, 2009; Klein et al., 2013) at temperatures below 315–350 °C, the amount of magnetite formation increases with increasing temperature (Fig. 7). By contrast, it

Please cite this article in press as: Ueda, H., et al., Reactions between olivine and CO_2-rich seawater at 300 °C: Implications for H_2 generation and CO_2 sequestration on the early Earth, Geoscience Frontiers (2016), http://dx.doi.org/10.1016/j.gsf.2016.10.002

Table 3
Composition of run products (wt.%).

Sample	Olivine		Magnesite			Dolomite	Serpentine			Magnetite		Brucite	
SiO_2	40.74	40.87	0.13	0.00	0.00	0.00	38.77	37.44	39.67	2.18	3.66	0.04	0.08
TiO_2	0.00	0.00	0.00	0.00	0.00	0.00	0.00	0.00	0.00	0.00	0.00	0.00	0.00
Al_2O_3	0.03	0.03	0.06	0.00	0.01	0.00	0.12	0.11	0.03	0.01	0.02	0.22	0.01
Cr_2O_3	0.03	0.03	0.02	0.05	0.00	0.01	0.03	0.00	0.00	0.00	0.03	0.00	0.00
FeO_{total}[a]	8.43	8.25	2.08	8.56	6.22	0.64	1.79	2.14	8.21	86.17	84.87	8.25	5.67
MnO	0.12	0.16	1.17	0.66	0.69	1.15	0.05	0.01	0.05	0.31	0.08	0.30	0.34
MgO	50.11	49.59	38.20	35.26	39.32	19.76	31.41	32.65	40.56	2.23	2.05	62.22	63.29
CaO	0.05	0.07	3.00	1.90	2.05	27.31	0.00	0.01	0.06	0.00	0.00	0.00	0.00
Na_2O	0.02	0.01	0.02	0.04	0.04	0.01	0.08	0.03	0.01	0.03	0.08	0.03	0.00
K_2O	0.04	0.04	0.16	0.12	0.10	0.21	0.12	0.04	0.05	0.09	0.00	0.00	0.00
NiO	0.33	0.39	0.00	0.04	0.08	0.03	0.22	0.22	0.30	0.47	1.07	0.15	0.08
Total	99.89	99.45	44.83	46.61	48.51	49.12	72.59	72.66	88.92	91.50	91.85	71.19	69.47
$Mg^{\#}$[b]	91.37	91.46	97.03	88.02	91.85	98.22	96.90	96.45	89.80	4.41	4.13	93.08	95.22

[a] Total iron as FeO.
[b] $Mg^{\#} = [Mg/(Mg + Fe)] \times 100$.

drastically decreases at temperatures above 315–350 °C because olivine becomes stable, which is unfavorable for H_2 generation. Little carbonate mineral was formed via the reaction between the olivine and the CO_2-rich fluid (20 mmol/kg) at 320 °C (McCollom et al., 2016), but this is likely attributable to the amount of reacted olivine (approximately 2.7%) and the resulting negligible alkaline metal element concentrations in the fluids. Conversely, the reaction between the komatiite and the CO_2-rich fluid (400 mmol/kg) at 350 °C precipitates a certain amount of carbonate minerals, even though it is calcite containing little ferrous iron (Ueda et al., 2016). Therefore, it remains uncertain whether CO_2-rich fluid suppresses hydrogen generation in ultramafic systems over 300 °C or not.

5. Implications for CO_2 sequestration to the mantle and H_2 production on the early Earth

Geological records suggest that the atmospheric CO_2 level in the Archean was much higher than the modern equivalent (Lowe and Tice, 2004; Ohmoto et al., 2004; Shibuya et al., 2007, 2012). Moreover, theoretical calculations suggest that a large quantity of CO_2 existed in the ocean-atmosphere system on the early Earth compared to modern levels (e.g., Walker, 1985; Kasting, 1993; Zahnle et al., 2007, 2010), which is further supported by the amount of fixed carbon as sedimentary rocks on the surface (Ronov and Yaroshevsky, 1967, 1969). The early atmosphere may have contained all the Earth's carbon, which would correspond to a partial pressure of CO_2 on the order of 10–340 MPa (Liu, 2004; Elkins-Tanton, 2008). Unlike present Earth, continental carbonate rocks could not be a sufficient reservoir of CO_2 because pervasive continents on the early Earth would have been rare. Therefore, mechanisms are required to transport an enormous amount of surface CO_2 into the Earth's interior into temporal reservoirs.

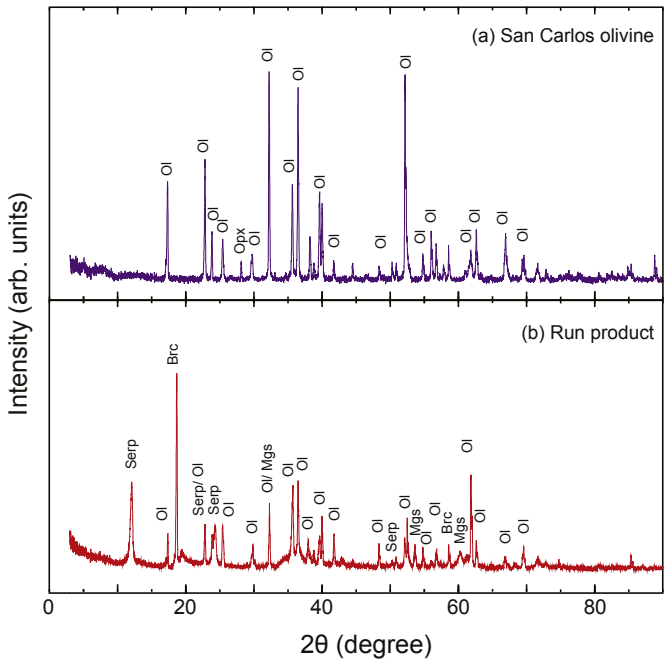

Figure 5. Representative XRD patterns (CuKα) of (a) the unaltered San Carlos olivine and (b) the alteration products formed in this hydrothermal experiment. Mgs: Magnesite, Ol: Olivine, Serp: Serpentine, Brc: Brucite, and Opx: Orthopyroxene.

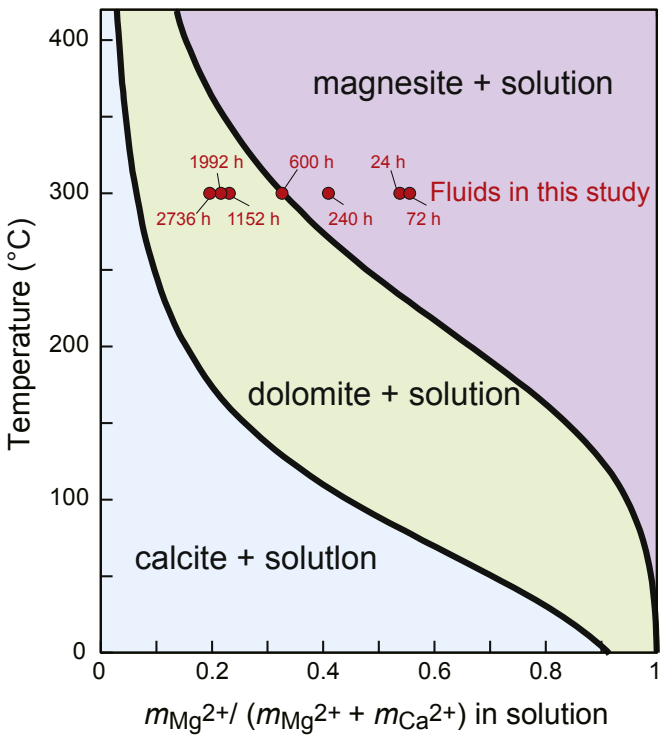

Figure 6. Calcite-dolomite-magnesite stability fields as functions of the temperature and the $m_{Mg^{2+}}/(m_{Mg^{2+}} + m_{Ca^{2+}})$ value estimated from experiments at 275–420 °C and their extrapolation to 0 °C (modified after Tribble et al., 1995). The solid curves indicate the solutions with 1 M of Ca-Mg chloride. The range of hydrothermal fluids in this study is plotted as a red bar.

Please cite this article in press as: Ueda, H., et al., Reactions between olivine and CO_2-rich seawater at 300 °C: Implications for H_2 generation and CO_2 sequestration on the early Earth, Geoscience Frontiers (2016), http://dx.doi.org/10.1016/j.gsf.2016.10.002

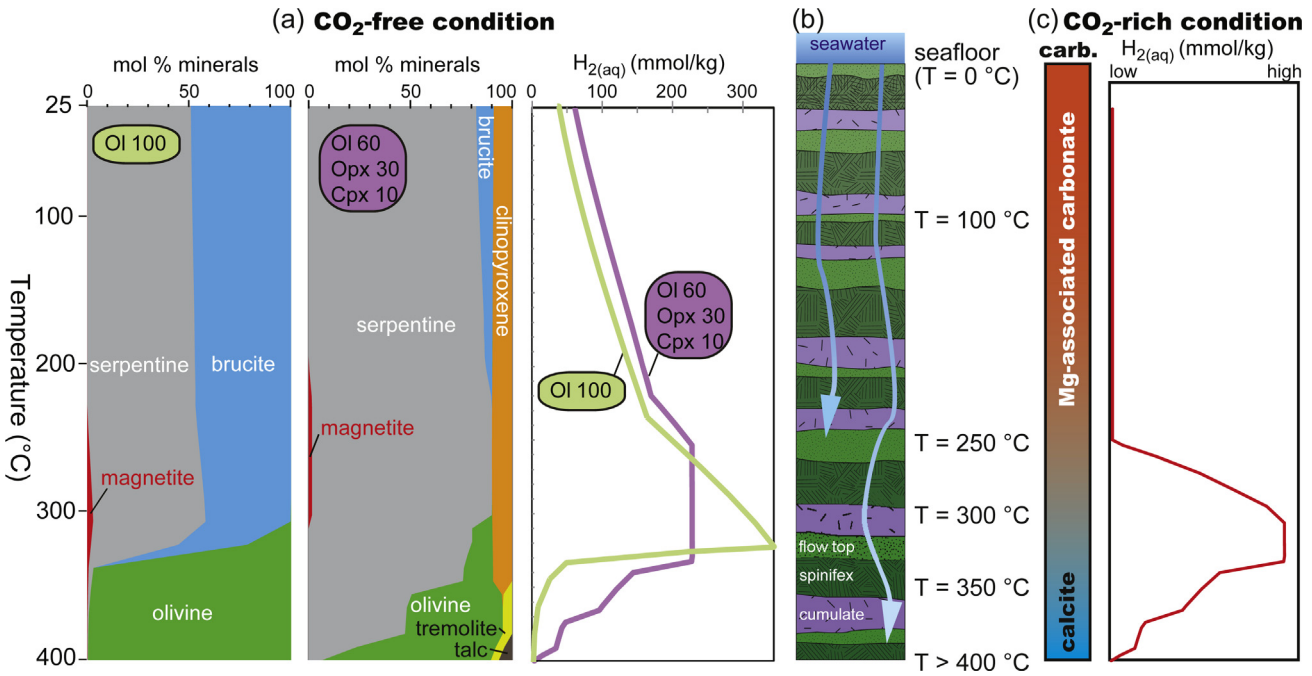

Figure 7. (a) Mineral assemblages and amounts of H_2 production formed via serpentinization of olivine and the representative peridotite as a function of temperature based on thermodynamic calculations (Klein et al., 2013). (b) Schematic of the carbonated komatiite crust on the early Earth. (c) Predicted carbonate mineralogy and speculated H_2 concentration in fluids formed via serpentinization under CO_2-rich conditions as a function of temperature. See Section 5 for details.

Subduction of carbonated basaltic oceanic crust has been considered as one of the important carrier of CO_2 (e.g., Sleep and Zahnle, 2001; Dasgupta and Hirschmann, 2010). However, difficulties in using this process arise from the hot temperature-depth trajectories of the subduction zones on the early Earth (Maruyama et al., 1996), where all the CO_2 fixed in the basaltic oceanic crust as carbonate minerals could be released before the crust reached the Moho boundary (Aral et al., this volume). In contrast, Mg-bearing carbonate minerals (e.g., dolomite and magnesite) formed in ultramafic rocks could survive this shallow release and may pass through the Moho boundary due to their wide stability fields (Aral et al., this volume). Moreover, Dasgupta and Hirschmann (2010) indicated that hydrothermally altered peridotite (ophicarbonate) in subducting plates could reach greater depths into the interior against the decarbonation.

Based on geological records, Archean oceanic crust was likely much thicker than modern equivalents due to the higher potential mantle temperature at that time (Fig. 1; Ohta et al., 1996; Komiya et al., 2002; Moores, 2002; Komiya, 2004). Such thick oceanic crusts presumably prevented the exposure of mantle peridotites on the seafloor. The high potential mantle temperature likely induced more frequent hotspot-like komatiite volcanism; therefore, komatiite would have been exposed to hydrothermal fluids much more abundant than peridotites on the early Earth.

Experimental studies of CO_2-rich basalt-hosted hydrothermal systems have demonstrated that only calcite is formed as a major carbonate mineral at 250 °C and 350 °C (Shibuya et al., 2013). Whereas, experimental studies of CO_2-rich komatiite-hosted hydrothermal systems have demonstrated that the precipitated carbonate species are ferroan dolomite at 250 °C and calcite at 350 °C and 500 bars (Ueda et al., 2016), ferroan dolomite or magnesian calcite at 300 °C and 500 bars (Hao and Li, 2015), and calcite at 300 °C and 350 bars (Lazar et al., 2012). The difference in carbonate mineralogy at 300 °C may arise from the initial ΣCO_2 concentrations of the fluids, which are 1600 mmol/kg (Hao and Li, 2015) and 80 mmol/kg (Lazar et al., 2012), respectively. Considering these results, the precipitated carbonate mineralogy in CO_2-rich komatiite-hosted hydrothermal systems is possibly classified into (1) Mg-associated carbonate below approximately 300 °C and (2) calcite over approximately 300 °C (Fig. 7c). This has important implications for the surface environment on the early Earth, as discussed below.

Carbonate mineralogy formed by water/rock reactions potentially affects the CO_2 influx from the ocean-atmosphere system to the mantle on the early Earth. Oceanic crusts that once experienced carbonation via hydrothermal circulation more or less suffer decarbonation in the subduction zone (Fig. 1). According to thermodynamic calculations (Arai et al., this volume), Mg-bearing carbonate minerals can survive CO_2 degassing even under the hot P-T conditions of subduction zones on the early Earth. As mentioned, hydrothermal reactions between komatiite and CO_2-rich fluids precipitate dolomite at temperature below 300 °C. In the following, we roughly estimate the maximum amount of CO_2 transported into the deep mantle by the subduction of dolomite-containing komatiite.

In the Phanerozoic, volumetric volcanic output rates of flood basalt have been estimated to be on the order of 1 km^3/year (White et al., 2006). We made the provisional assumption that the successive komatiite volcanism formed, on average, a 4 km-thick komatiite crust on the basaltic oceanic crust on the early Earth (Fig. 1). When applying similar volcanic output rates of modern hotspots to the early Earth, this is equal to an annual production rate of 2.5×10^{-1} km^2 komatiite on the whole. Geological records of the Archean, carbonate formation via hydrothermal alteration extended to a depth of 4 km (Shibuya et al., 2012), but the temperature range that allowed dolomite formation (approximately 300 °C) was limited to the upper 3 km. Shibuya et al. (2012) reported that the average amount of fixed CO_2 per unit area of seafloor was approximately 1.2×10^{13} mol/km^2, based on the volume concentrations of carbonate minerals in Archean basaltic crusts. Hypothetically speaking, if all the fixed carbon as dolomite in the komatiite crust could be subducted into the deep mantle without

Please cite this article in press as: Ueda, H., et al., Reactions between olivine and CO_2-rich seawater at 300 °C: Implications for H_2 generation and CO_2 sequestration on the early Earth, Geoscience Frontiers (2016), http://dx.doi.org/10.1016/j.gsf.2016.10.002

any degassing, 2.8×10^{12} mol of CO_2 would be removed annually from the ocean-atmosphere system. In other words, this means that 1.4×10^{21} mol of CO_2 (roughly equivalent to 8% of 100 bars of CO_2 atmosphere) was sequestered within the Hadean. Volcanic activities on the early Earth are vaguely considered to have been much higher than that at present. Even though these estimations are highly speculative, we consider that the subduction of the Mg-bearing carbonate formed in komatiite likely transported significant amounts of surface CO_2 into the deep mantle, even in hot subduction zones.

The amount of H_2 production in komatiite-hosted hydrothermal systems could be reduced under CO_2-rich conditions below approximately 300 °C due to the formation of Mg-bearing carbonate minerals. Fe is generally predisposed to substitute for Mg in natural systems. Ferrous iron incorporation into carbonate minerals likely limits iron oxidation, which must be unfavorable to H_2 generation. In fact, dolomite grains formed in komatiite-hosted hydrothermal systems at 250 °C contain certain amounts of ferrous iron (up to 9 wt.% as FeO), and the resulting maximum H_2 concentration for such a system was only approximately 0.024 mmol/kg (Ueda et al., 2016). Such a trend can be extrapolated into low-temperature regions down to 70 °C based on the results of hydrothermal experiments using olivine (Jones et al., 2010; Klein and McCollom, 2013; Neubeck et al., 2014). In addition, the potential for H_2 generation in ultramafic systems decreases with decreasing temperature by thermodynamic calculations (Fig. 7a; McCollom and Bach, 2009; Klein et al., 2013), and carbonate minerals become more stable in such low temperature conditions (Shibuya et al., 2013; Ueda et al., 2016). Therefore, H_2 concentrations in fluids formed below 250 °C could be negligible (Fig. 7c). At 300 °C, carbonate precipitation likely reduces H_2 production in some degree (Hao and Li, 2015; this study), but H_2 concentration in fluids could still be high compared to other temperature ranges due to the temperature dependency of the stability of magnetite (Fig. 7a). On the other hand, calcite is formed in CO_2-rich komatiite hydrothermal systems above approximately 300 °C (Lazar et al., 2012; Ueda et al., 2016). Because the calcite has little influence on H_2 generation owing to its low ferrous iron content, H_2 concentrations in fluids above 300 °C are almost similar to those formed in a CO_2-free system (Fig. 7a and c). Therefore, even under CO_2-rich conditions, the amount of H_2 was high at high temperatures (>approximately 300 °C). Such high H_2-rich fluids could be important to sustain early ecosystems (Maruyama et al., 2016).

6. Summary and conclusions

We conducted a hydrothermal alteration experiment to monitor the reaction between olivine and a CO_2-rich NaCl solution at 300 °C and 500 bars. The H_2 concentration reached up to approximately 39 mmol/kg within 2736 h, which is relatively lower than the concentration formed under a CO_2-free condition. This phenomenon is likely attributable to ferrous iron incorporation into Mg-bearing carbonate minerals because such a substitution prevents iron oxidation in fluids. Considering the results obtained from previous hydrothermal experiments using olivine and ultramafic rocks, the hydrothermally precipitated carbonate species in ultramafic systems are the Mg-bearing carbonates below 300 °C, but calcite above 300 °C. This suggests that only high-temperature komatiite-hosted hydrothermal systems have the potential for generating H_2-rich hydrothermal fluids, even in CO_2-abundant early ocean-atmosphere systems. Further hydrothermal experiments using komatiite should be conducted at temperatures near 300 °C under more realistic CO_2 levels to simulate the early ocean-atmosphere system because this study demonstrated that the ΣCO_2 concentration in the fluid may be sensitive to the carbonate mineralogy and the resulting H_2 generation for a given temperature range.

Acknowledgments

We thank an anonymous reviewer for their comments and Prof. M. Santosh for his editorial handling. We thank Yoko Ohtsuka for technical advice (ICP-OES) at the Center for Advanced Materials Analysis in the Tokyo Institute of Technology, Japan and Dr. Hisashi Asanuma for acquiring the chemical composition with EPMA. This work was partly supported by a grant for "Hadean BioScience (No. 26106002)" from the Ministry of Education, Culture, Sports, Science and Technology, Japan.

References

Allen, D.E., Seyfried Jr., W.E., 2003. Compositional controls on vent fluids from ultramafic-hosted hydrothermal systems at mid-ocean ridges: an experimental study at 400 °C, 500 bars. Geochimica et Cosmochimica Acta 67, 1531–1542.

Amend, J.P., McCollom, T.M., 2009. Energetics of biomolecule synthesis on early Earth. In: Zaikowski, L., Friedrich, J.M., Seidel, S.R. (Eds.), Chemical Evolution II: From the Origins of Life to Modern Society, American Chemical Society Symposium Series. Oxford University Press, New York, pp. 63–94.

Arai, T., Omori, S., Komiya, T., Maruyama, S., submitted to this volume. Metamorphic Decarbonation of Oceanic Crust at the Subduction Zone in Early Earth: Implications for Carbon Cycle in the Early Earth.

Berndt, M.E., Allen, D.E., Seyfried, W.E., 1996. Reduction of CO_2 during serpentinization of olivine at 300 °C and 500 bar. Geology 24, 351–354.

Charlou, J.L., Donval, J.P., Fouquet, Y., Jean-Baptiste, P., Holm, N., 2002. Geochemistry of high H_2 and CH_4 vent fluids issuing from ultramafic rocks at the Rainbow Hydrothermal Field (36°14Ń, MAR). Chemical Geology 191, 345–359.

Charlou, J.L., Donval, J.P., Konn, C., Ondreas, H., Fouquet, Y., Jean-Baptiste, P., Fourre, E., 2010. High production and fluxes of H_2 and CH_4 and evidence of abiotic hydrocarbon synthesis by serpentinization in ultramafic-hosted hydrothermal systems on the Mid-Atlantic Ridge. In: Rona, P., Devey, C., Dyment, J., Murton, B. (Eds.), Diversity of Hydrothermal Systems on Slow-spreading Ocean Ridges, Geophysical Monograph Series, vol. 188. 440 pp., hardbound. ISBN 978-0-87590-478-8, AGU Code GM1884788.

Connolly, J.A.D., 2005. Computation of phase equilibria by linear programming: a tool for geodynamic modeling and its application to subduction zone decarbonation. Earth and Planetary Science Letters 236, 524–541.

Dasgupta, R., Hirschmann, M.M., 2010. The deep carbon cycle and melting in Earth's interior. Earth and Planetary Science Letters 298, 1–13.

Dasgupta, R., Hirschmann, M.M., Dellas, N., 2005. The effect of bulk composition on the solidus of carbonated eclogite from partial melting experiments at 3 GPa. Contributions to Mineralogy and Petrology 149, 288–305.

Elkins-Tanton, L.T., 2008. Linked magma ocean solidification and atmospheric growth for Earth and Mars. Earth and Planetary Science Letters 271, 181–191.

Etiope, G., Schoell, M., Hosgörmez, H., 2011. Abiotic methane flux from the Chimaera seep and Tekirova ophiolites (Turkey): understanding gas exhalation from low temperature serpentinization and implications for Mars. Earth and Planetary Science Letters 310, 96–104.

Etiope, G., Sherwood Lollar, B., 2013. Abiotic methane on Earth. Reviews of Geophysics 51, 276–299.

Etiope, G., Vadillo, I., Whiticar, M.J., Marques, J.M., Carreira, P.M., Tiago, I., Benavente, J., Jiménes, P., Urresti, B., 2016. Abiotic methane seepage in the Ronda peridotite massif, southern Spain. Applied Geochemistry 66, 101–113.

Hao, X., Li, Y., 2015. Hexagonal plate-like magnetite nanocrystals produced in komatiite-H_2O-CO_2 reaction system at 450 °C. International Journal of Astrobiology 14, 547–553.

Hövelmann, J., Putnis, C.V., Ruiz-Agudo, E., Austrheim, H., 2012. Direct nanoscale observations of CO_2 sequestration during brucite [$Mg(OH)_2$] dissolution. Environmental Science & Technology 46, 5253–5260.

Jones, L.C., Rosenbauer, R., Goldsmith, J.I., Oze, C., 2010. Carbonate control of H_2 and CH_4 production in serpentinization systems at elevated P-Ts. Geophysical Research Letters 37, L14306.

Kasting, J.F., 1993. Earth's early atmosphere. Science 259, 920–926.

Kerrick, D.M., Connolly, J.A.D., 2001. Metamorphic devolatilization of subducted oceanic metabasalts: implications for seismicity, arc magmatism and volatile recycling. Earth and Planetary Science Letters 189, 19–29.

Klein, F., McCollom, T.M., 2013. From serpentinization to carbonation: new insights from a CO_2 injection experiment. Earth and Planetary Science Letters 379, 137–145.

Klein, F., Bach, W., McCollom, T.M., 2013. Compositional controls on hydrogen generation during serpentinization of ultramafic rocks. Lithos 178, 55–69.

Komiya, T., Maruyama, S., Hirata, T., Yurimoto, H., 2002. Petrology and geochemistry of MORB and OIB in the mid-Archean North Pole region, Pilbara Craton,

Please cite this article in press as: Ueda, H., et al., Reactions between olivine and CO_2-rich seawater at 300 °C: Implications for H_2 generation and CO_2 sequestration on the early Earth, Geoscience Frontiers (2016), http://dx.doi.org/10.1016/j.gsf.2016.10.002

Western Australia, implications for the composition and temperature of the upper mantle at 3.5 Ga. International Geology Review 44, 988–1016.
Komiya, T., 2004. Material circulation model including chemical differentiation within the mantle and secular variation of temperature and composition of the mantle. Physics of the Earth and Planetary Interiors 146, 333–367.
Lazar, C., McCollom, T.M., Manning, C.E., 2012. Abiogenic methanogenesis during experimental komatiite serpentinization: implications for the evolution of the early Precambrian atmosphere. Chemical Geology 326–327, 102–112.
Liu, L.-G., 2004. The inception of the oceans and CO_2-atmosphere in the early history of the Earth. Earth and Planetary Science Letters 227, 179–184.
Lowe, D.R., Tice, M.M., 2004. Geologic evidence for Archean atmospheric and climatic evolution: fluctuating levels of CO_2, CH_4, and O_2 with an overriding tectonic control. Geology 32, 493–496.
Macleod, G., McKeown, C., Hall, A.J., Russell, M.J., 1994. Hydrothermal and oceanic pH conditions of possible relevance to the origin of life. Origins of Life and Evolution of the Biosphere 24, 19–41.
Maruyama, S., Liou, J.G., Terabayashi, M., 1996. Blueschists and eclogites of the world and their exhumation. International Geology Review 38, 485–594.
Maruyama, S., Santosh, M., Sawaki, S., 2016. Birth Place of Life: not MOR but Geyser Driven by Natural Nuclear Reactor (submitted).
McCollom, T.M., Bach, W., 2009. Thermodynamic constraints on hydrogen generation during serpentinization of ultramafic rocks. Geochimica et Cosmochimica Acta 73, 856–875.
McCollom, T.M., Klein, F., Robbins, M., Moskowitz, B., Berquó, T.S., Jöns, N., Bach, W., Templeton, A., 2016. Temperature trends for reaction rates, hydrogen generation, and partitioning of iron during experimental serpentinization of olivine. Geochimica et Cosmochimica Acta 181, 175–200.
Molina, J.F., Poli, S., 2000. Carbonate stability and fluid composition in subducted oceanic crust: an experimental study on H_2O-CO_2-bearing basalts. Earth and Planetary Science Letters 176, 295–310.
Moores, E.M., 2002. Pre-1 Ga (pre-Rodinian) ophiolites: their tectonic and environmental implications. Geological Society of America, Bulletin 114, 80–95.
Neal, C., Stanger, G., 1983. Hydrogen generation from mantle source rocks in Oman. Earth and Planetary Science Letters 66, 315–320.
Neubeck, A., Duc, N.T., Hellevang, H., Oze, C., Bastviken, D., Bacsik, Z., Holm, N.G., 2014. Olivine alteration and H_2 production in carbonate-rich, low temperature aqueous environments. Planetary and Space Science 96, 51–61.
Neubeck, A., Nguyen, D.T., Etiope, G., 2016. Low-temperature dunite hydration: evaluating CH_4 and H_2 production from H_2O and CO_2. Geofluids 16 (3), 408–420.
Ohmoto, H., Watanabe, Y., Kumazawa, K., 2004. Evidence from massive siderite beds for a CO_2-rich atmosphere before ~1.8 billion years ago. Nature 429, 395–399.
Ohta, H., Maruyama, S., Takahashi, E., Watanabe, Y., Kato, Y., 1996. Field occurrence, geochemistry and petrogenesis of the Archean mid-oceanic ridge basalts (AMORBs) of the Cleaverville area, Pilbara Craton, Western Australia. Lithos 37, 199–221.
Oze, C., Sharma, M., 2005. Have olivine, will gas: serpentinization and the abiogenic production of methane on Mars. Geophysical Research Letters 32, L10203.
Poli, S., Franzolin, E., Fumagalli, P., Crottini, A., 2009. The transport of carbon and hydrogen in subducted oceanic crust: an experimental study to 5 GPa. Earth and Planetary Science Letters 278, 350–360.
Proskurowski, G., Lilley, M.D., Olson, E.J., 2008. Stable isotopic evidence in support of active microbial methane cycling in low-temperature diffuse flow vents at 9°50′ N East Pacific Rise. Geochimica et Cosmochimica Acta 72, 2005–2023.
Ronov, A.B., Yaroshevsky, A.A., 1967. Geochemistry 11, 1041–1066 (Translated from Geokhimiya 11, 1285, 1967.).
Ronov, A.B., Yaroshevsky, A.A., 1969. In: Hart, P.J. (Ed.), The Earth's Crust and Upper Mantle, Am. Geophys. Union Monograph 13, p. 37. Washington.
Ronov, A.B., 1964. Obshchie tendentsii v evolyutsii sostava zemnoj kory, okeana i atmosfery. Geokhimiya 8, 715–743.
Rosenberg, P.E., Holland, H.D., 1964. Calcite-dolomite-magnesite stability relations in solutions at elevated temperatures. Science 145, 700–701.
Rosenberg, P.E., Burt, D.M., Holland, H.D., 1967. Calcite-dolomite-magnesite stability relations in solutions: the effect of ionic strength. Geochimica et Cosmochimica Acta 31, 391–396.
Russell, M.J., Barge, L.M., Bhartia, R., Bocanegra, D., Bracher, P.J., Branscomb, E., Kidd, R., McGlynn, S., Meier, D.H., Nitschke, W., Shibuya, T., Vance, S., White, L., Kanik, I., 2014. The drive to life on wet and icy worlds. Astrobiology 14, 308–343.
Seyfried Jr., W.E., Gordon, P.C., Dickson, F.W., 1979. A new reaction cell for hydrothermal solution equipment. American Mineralogist 64, 646–649.
Seyfried Jr., W.E., Foustoukos, D.I., Fu, Q., 2007. Redox evolution and mass transfer during serpentinization: an experimental and theoretical study at 200 °C, 500 bar with implications for ultramafic-hosted hydrothermal systems at mid-ocean ridges. Geochimica et Cosmochimica Acta 71, 3872–3886.
Sleep, N.H., 2009. Stagnant lid convection and carbonate metasomatism of the deep continental lithosphere. Geochemistry, Geophysics, Geosystems 10.
Sleep, N.H., Zahnle, K., 2001. Carbon dioxide cycling and implications for climate on ancient Earth. Journal of Geophysical Research 106, 1373–1399.
Shibuya, T., Kitajima, K., Komiya, T., Terabayashi, M., Maruyama, S., 2007. Middle Archean ocean ridge hydrothermal metamorphism and alteration recorded in the Cleaverville area, Pilbara Craton, Western Australia. Journal of Metamorphic Geology 25, 751–767.
Shibuya, T., Tahata, M., Kitajima, K., Ueno, Y., Komiya, T., Yamamoto, S., Igisu, M., Terabayashi, M., Sawaki, Y., Takai, K., Yoshida, N., Maruyama, S., 2012. Depth variation of carbon and oxygen isotopes of calcites in Archean altered upper oceanic crust: implications for the CO_2 flux from ocean to oceanic crust in the Archean. Earth and Planetary Science Letters 321–322, 64–73.
Shibuya, T., Yoshizaki, M., Masaki, Y., Suzuki, K., Takai, K., Russell, M.J., 2013. Reactions between basalt and CO_2-rich seawater at 250 and 350 °C, 500 bars: implications for the CO_2 sequestration into the modern oceanic crust and the composition of hydrothermal vent fluid in the CO_2-rich early ocean. Chemical Geology 359, 1–9.
Shibuya, T., Yoshizaki, M., Satoh, M., Shimizu, K., Nakamura, K., Omori, S., Suzuki, K., Takai, K., Hideo, T., Maruyama, S., 2015. Hydrogen-rich hydrothermal environments in the Hadean ocean inferred from serpentinization of komatiites at 300 °C and 500 bar. Progress in Earth and Planetary Science 2, 1–11.
Tribble, J.S., Arvidson, R.S., Lane, M., Mackenzie, F.T., 1995. Crystal chemistry, and thermodynamic and kinetic properties of calcite, dolomite, apatite, and biogenic silics: applications to petrographic problems. Sedimentary Geology 95, 11–51.
Ueda, H., Shibuya, T., Sawaki, Y., Saitoh, M., Takai, K., Maruyama, S., 2016. Reactions between Komatiite and CO_2-rich Seawater at 250 °C and 350 °C at 500 bars: Implications for Hydrogen Generation in the Hadean Seafloor Hydrothermal System (submitted).
Veizer, J., Mackenzie, F.T., Heinrich, D.H., Karl, K.T., 2003. Evolution of Sedimentary Rocks, Treatise on Geochemistry. Pergamon, Oxford, pp. 369–407.
Walker, J.C.G., 1985. Carbon dioxide on the early earth. Origins of Life and Evolution of the Biosphere 16, 117–127.
Wetzel, L.R., Shock, E.L., 2000. Distinguishing ultramafic- from basalt-hosted submarine hydrothermal systems by comparing calculated vent fluid compositions. Journal of Geophysical Research 105, 8319–8340.
White, S.M., Crisp, J.A., Spera, F.J., 2006. Long-term volumetric eruption rates and magma budgets. Geochemistry, Geophysics, Geosystems 7. http://dx.doi.org/10.1029/2005GC001002.
Yaxley, G.M., Green, D.H., 1994. Experimental demonstration of refractory carbonate-bearing eclogite and siliceous melt in the subduction regime. Earth and Planetary Science Letters 128, 313–325.
Yoshizaki, M., Shibuya, T., Suzuki, K., Shimizu, K., Nakamura, K., Takai, K., Omori, S., Maruyama, S., 2009. H_2 generation by experimental hydrothermal alteration of komatiitic glass at 300 °C and 500 bars: a preliminary result from on-going experiment. Geochemical Journal 43, e17–e22.
Zahnle, K., Arndt, N., Cockell, C., Halliday, A., Nisbet, E., Selsis, F., Sleep, N.H., 2007. Emergence of a Habitable Planet, Geology and Habitability of Terrestrial Planets, pp. 35–78.
Zahnle, K., Schaefer, L., Fegley, B., 2010. Earth's earliest atmosphere. Cold Spring Harbor Perspectives in Biology 2, a004895.
Zhao, L., Sang, L., Chen, J., Ji, J.F., Teng, H.H., 2010. Aqueous carbonation of natural brucite: relevance to CO_2 sequestration. Environmental Science & Technology 44, 406–411.

Please cite this article in press as: Ueda, H., et al., Reactions between olivine and CO_2-rich seawater at 300 °C: Implications for H_2 generation and CO_2 sequestration on the early Earth, Geoscience Frontiers (2016), http://dx.doi.org/10.1016/j.gsf.2016.10.002